GeoHazards

MDPI

Article

A Preliminary Hazard Assessment of Kolumbo Volcano (Santorini, Greece)

Anna Katsigera [1,*], Paraskevi Nomikou [1,*] and Kosmas Pavlopoulos [2]

[1] Department of Geology and Geoenvironment, National and Kapodistrian University of Athens, 157 72 Athens, Greece
[2] Geography and Planning Department, Sorbonne University, Abu Dhabi P.O. Box 38044, United Arab Emirates; kosmas.pavlopoulos@sorbonne.ae
* Correspondence: annakat@geol.uoa.gr (A.K.); evinom@geol.uoa.gr (P.N.)

Abstract: Volcanic eruptions stand as destructive threats to adjacent communities, unleashing multiple hazards such as earthquakes, tsunamis, pyroclastic flows, and toxic gases. The imperative for proactive management of volcanic risks and communities' adaptation cannot be overstated, particularly in densely populated areas where the potential for widespread devastation looms large. Kolumbo, an active submarine volcano located approximately 7 km northeast of Santorini Island in Greece, serves as a pertinent case. Its historical record is characterised by an eruption in 1650 CE that produced a catastrophic tsunami. The aftermath witnessed havoc on neighbouring islands, coupled with casualties stemming from noxious gases in Santorini. Eyewitness accounts mention maximum water run-up heights of 20 m on the southern coast of Ios, inundation of an area of 240 m inland on Sikinos, and a flooding of up to 2 km^2 inland on the eastern coast of Santorini. Recent studies suggest that a potential future eruption of Kolumbo poses a substantial hazard to the northern and eastern coasts of Santorini. Unfortunately, the absence of a concrete management protocol leaves these areas vulnerable to an impending threat that demands immediate attention. Therefore, it is recommended that a comprehensive approach be adopted, involving scientific research (active monitoring, hazard maps), community engagement, preparedness planning with government agencies, and the development of timely response strategies to reduce the associated risks, prevent casualties, and mitigate the potential consequences on the region's economy and infrastructure.

Keywords: volcanic hazards; hazard assessment; monitoring; submarine volcanism

check for updates

Citation: Katsigera, A.; Nomikou, P.; Pavlopoulos, K. A Preliminary Hazard Assessment of Kolumbo Volcano (Santorini, Greece). *GeoHazards* **2024**, *5*, 816–832. https://doi.org/10.3390/geohazards5030041

Academic Editors: Zhong Lu and Tiago Miguel Ferreira

Received: 29 May 2024
Revised: 12 August 2024
Accepted: 14 August 2024
Published: 19 August 2024

Copyright: © 2024 by the authors. Licensee MDPI, Basel, Switzerland. This article is an open access article distributed under the terms and conditions of the Creative Commons Attribution (CC BY) license (https://creativecommons.org/licenses/by/4.0/).

1. Introduction

Managing volcanic risk encompasses a multifaceted and crucial field aimed at reducing the hazards posed by volcanic eruptions to human life, infrastructure, and the surrounding environment. This includes preparedness planning, monitoring, and responsive actions. Initially, it involves continuous monitoring of volcanic activity using state-of-the-art technology and geophysical tools [1]. Subsequently, early warning systems are established to promptly alert vulnerable communities. Disaster preparedness and evacuation plans alongside public awareness campaigns facilitate effective responses during eruptions [2], while post-eruption actions ensure rapid restoration of vital services and infrastructure [3]. In essence, managing volcanic risk necessitates a comprehensive and cooperative strategy that integrates scientific research, policy formulation, and community engagement to mitigate the potential negative outcomes caused by volcanic eruptions.

Volcanic hazards are often interconnected and can lead to a number of negative impacts. Recent eruptions have shown that the multifaceted aspects of hazards need to be taken into consideration to minimise their impact on the environment, the human population, and regional and global economies. The 2010 eruption of Eyjafjallajökull, dormant for nearly 200 years, began with a small fissure eruption but escalated into an explosive subglacial event, producing significant ash that disrupted air traffic across Europe and caused

widespread economic losses and health issues [4–6]. The ash and volcanic gases posed respiratory risks and long-term health effects, while melting glacial ice generated lahars, threatening downstream communities [6]. This event highlighted the vulnerability of modern society to volcanic hazards, drawing comparisons to other multi-cascading hazard scenarios like the 2014 eruption of Mount Ontake [7] and the 2022 eruption of Hunga Tonga–Hunga Ha'apai [8].

Santorini island, located in the Aegean Sea, sustains a population of 15,550 [9]. Its neighbouring islands of Ios, Sikinos, and Anafi hold a population of 2024, 253, and 291, respectively [9]. The region is a famous tourist hotspot, with millions of visitors during the summer—especially in Santorini, whose number reach approximately 2 million. Most inhabitants are engaged in tourism-related occupations, with only a minority involved in traditional pursuits such as fishing and viniculture [10]. The economic stability of the entire populace hangs precariously in the balance, vulnerable to the potential repercussions of a volcanic eruption of Kolumbo in the future, which could profoundly impact local infrastructure and the economy of Santorini and other nearby island communities.

Kolumbo, located 7 km NE of Santorini, is an underwater active volcano [11]. Its eruption in 1650 CE triggered a devastating tsunami and emitted toxic gases, resulting in casualties and extensive damage in Santorini [12]. Recent studies indicate that a potential eruption could pose a significant threat to the eastern coast of Santorini [13], yet there exists no established management protocol for such an event. In this study, we present preliminary results of hazard zonation in Santorini. For the first time, semi-automated techniques were used and combined with optical qualitative data and historical observations to characterise the structure and hazard risks of Kolumbo's crater, an area that is otherwise unknown in terms of hazard assessments. We propose a comprehensive strategy based on scientific research, including active monitoring and hazard mapping, community engagement initiatives, collaboration with governmental bodies such as Civil Protection, and the implementation of rapid response measures. This multifaceted approach aims to mitigate volcanic hazards, avert casualties, and safeguard the region's economy and infrastructure.

1.1. Geological Setting

The Hellenic Volcanic Arc (HVA), stretching over 450 km, marks the zone where the African plate subducts beneath the Aegean microplate [14,15]. Since the Oligocene-Miocene period, there has been a regional extension, which has been facilitated by both pre-existing E-W oriented faults and newer NE-SW oriented normal faults that continue to be tectonically active today [16].

Situated within the HVA, the Christiana–Santorini–Kolumbo volcanic field (CSK) ranks among the most hazardous volcanic regions globally, with over 100 explosive eruptions recorded in the past 650,000 years [16]. The CSK (Figure 1) is situated along a 60 km-long rift zone oriented southwest to northeast, housing the Christiana volcano, the Santorini caldera, the submerged Kolumbo volcano (Figure 2), and the Kolumbo volcanic chain, comprising 24 underwater cones [17,18]. Santorini has experienced at least four significant caldera-forming eruptions, with the most recent, known as the "Minoan" eruption, occurring approximately 3600 years ago, recognised as one of the largest volcanic events during the Holocene for this volcanic suite [16,19]. This eruption is believed to have had substantial repercussions on human populations in the eastern Mediterranean region, potentially contributing to the downfall of the Minoan Civilization [20].

Piper et al. [22] proposed that volcanic activity in the CSK volcanic field commenced at Christiana during the early Pleistocene, with a peak phase of activity around 0.6 Ma. In this case, the entire Kolumbo edifice represents a recent volcanic episode contemporaneous with the Thera Pyroclastic Formation (<0.36 Ma) at Santorini [18]. However, subsequent studies indicate that the Kolumbo volcano is more complex than previously presumed, comprising five stacked volcanoclastic units from distinct eruptive cycles, for which two disparate chronologies suggesting significantly different ages for the onset of Kolumbo volcanism

(180 Ka versus 1.6 Ma) have been proposed [23]. This underscores substantial uncertainty in the chronological framework of the volcanic field, complicating the comprehension of volcano–tectonic interactions in a densely populated region where volcanic hazard assessment is considered essential. Kolumbo's edifice has been shaped by multiple eruptive cycles over more than 1 Myrs [18]. The most recent eruption occurred in 1650 CE, resulting in the formation of a cone comprised of stratified pumice deposits reaching approximately 260 m in thickness. This eruption breached the sea surface, but the cone was subsequently destroyed by a violent explosive event, forming a crater measuring 500 m in depth and 2500 m in width [24].

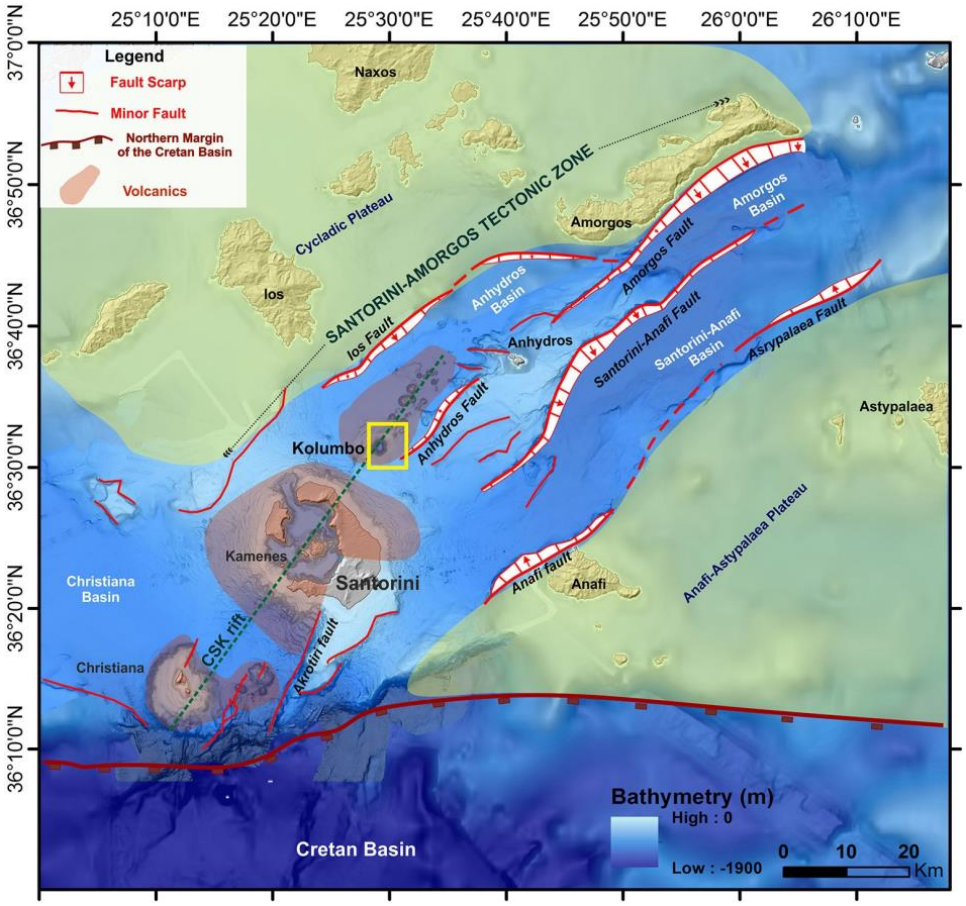

Figure 1. The Christiana–Santorini–Kolumbo rift showing the location of active and recent volcanic centres. Image modified from [17] with permission. The Kolumbo submarine volcano is indicated in the yellow box.

Recent oceanographic expeditions utilising high-resolution bathymetry data and optical observations have unveiled the morphological characteristics of Kolumbo's crater [21]. The cone formed during the 1650 CE eruption is predominantly composed of highly vesicular pumice, deposited as fallout from the eruption column (Figure 3). Many large pumice clasts floated on the sea surface before eventually sinking [25]. This cone, with a volume estimated at approximately 5 to 7 km^3, was formed within a remarkably brief period of just two weeks, according to eyewitness reports [26]. The northern section of Kolumbo crater's seafloor is home to both high-temperature (up to 220 °C) and low-temperature (up to 70 °C) polymetallic chimneys and hydrothermal vents, often adorned with bacterial colonies [27,28].

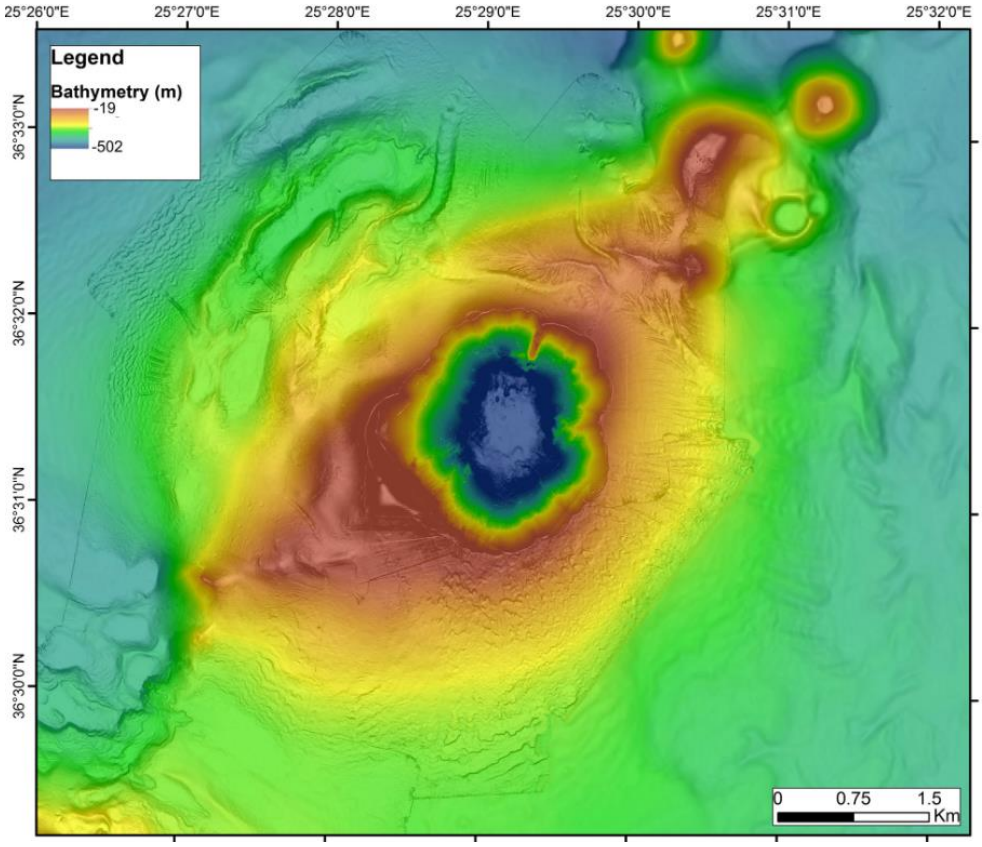

Figure 2. High−resolution map of the Kolumbo volcano. Bathymetric data were collected by GEOMAR's autonomous underwater vehicle (AUV) Abyss during mission POS 510 [21] with permission.

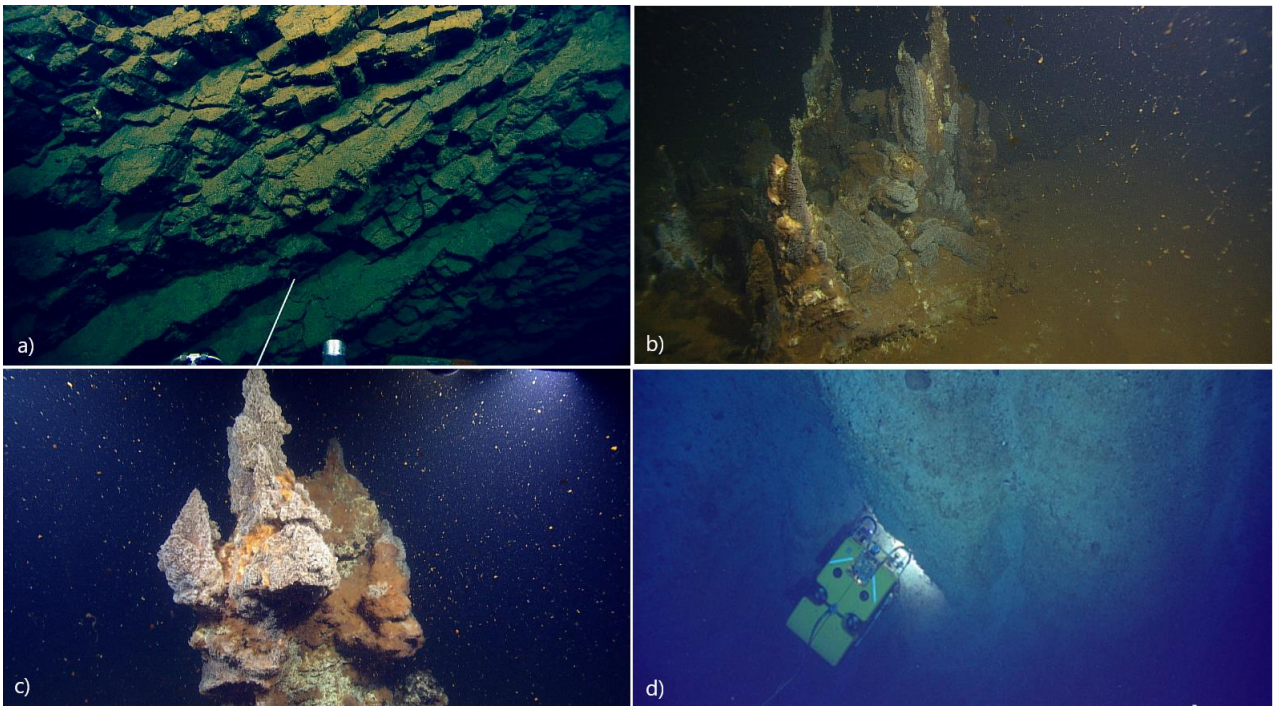

Figure 3. Remotely operated vehicle (ROV) captures from dives in the Kolumbo crater in expedition NA007 with E/V Nautilus. Images obtained from [29] with permission. Captures show (**a**) a lava dyke, (**b**,**c**) hydrothermal chimneys, and (**d**) pumice deposits.

1.2. The 1650 CE Eruption

In 1650 CE, Kolumbo experienced a series of explosive eruptions, extensively documented by Fouqué [12]. The initial phase of the eruption began in September 1650 CE, marked by violent seismic activity and subterranean roaring starting on the 14th and persisting throughout the month. Subaerial activity began on the 27th, with plumes repeatedly breaking the sea surface above the cone. Volcanic gases inundated the archipelago, and a small islet formed just above the surface. Small earthquakes persisted, large quantities of pumice were produced, and plumes formed and dispersed on an approximately hourly cycle throughout the 28th.

On 29 September, 1650 CE, the eruption reached its most violent phase. The subaerial plume that had formed on the 28th remained visible as incandescent material was seen being ejected from the crater. Lightning within the plume was accompanied by explosions heard as far as 400 km away in the Dardanelles. Intense earthquakes increased in frequency and were felt in Crete, while ash fallout from the plume reached mainland Turkey.

Santorini experienced at least one tsunami generated by the eruption, resulting in the destruction of buildings, erosion of roadways, and submergence of approximately 2.02 km of land along the eastern coastline. The tsunami also affected the islands of Ios, reaching 20 m inland, and Sikinos, reaching 32 m inland, causing significant damage. Local communities faced various hazards, including toxic gas clouds released during the eruptions, resulting in health issues such as eye pain, blindness, and cerebral congestion. Over 70 individuals succumbed to asphyxiation, and numerous animals perished. Furthermore, on the night of 2 October, the nine-man crew of a ship passing near Kolumbo were asphyxiated, while the crew of a nearby ship lost consciousness but survived. Reports indicated that the gases also caused discoloration of coins, sacred vessels in churches, paintings, and building walls.

Following a few days of decreased activity, the eruption began to wane. Isolated plume-forming events occurred on 4 and 5 November, accompanied by gas release and minor earthquakes. Despite an increase in earthquake intensity and submarine disturbances in early December, the 1650 CE eruption of Kolumbo came to an end. Small shocks and elevated water temperatures around Kolumbo persisted for several years, but the small edifice eroded beneath the waves within a few months.

The precise mechanisms underlying the 1650 CE tsunami have been a subject of debate due to the complexity and the limitations of submarine environments. Recent studies, however, have shown that approximately 1.2 km^3 of Kolumbo's northwestern flank experienced a downward movement of 500–1000 m along a basal detachment surface that led to the depressurization of the magma feeding system and subsequent explosion [1]. Through numerical tsunami simulations, Karstens et al. [13] demonstrated that the historical eyewitness testimonies can only be reconciled by the sequential occurrence of flank movement followed by an explosive eruption.

2. Materials and Methods

Effectively managing volcanic risk necessitates a multifaceted, interdisciplinary approach that integrates scientific expertise, risk evaluation, community preparedness, and emergency response planning. This comprehensive risk management strategy encompasses hazard assessment, which involves identifying volcanic threats associated with the volcano in question. Utilising historical eruption data provides valuable insights into eruption frequency, intensity, and patterns, thereby enhancing our comprehension of the volcano's behaviour and regional volcanic history [30].

A wealth of multidisciplinary data from past oceanographic expeditions were collected that help us understand Kolumbo's behaviour. These include (a) high-resolution multibeam bathymetry data and optical data; (b) a dense network of sub-seafloor seismic reflection profiles; (c) a series of seafloor and sub-seafloor samples of microbial mat and sediments; (d) conductivity, temperature, and depth (CTD) data; (e) several polymetallic (Au, Ag, As, Sb, Pb, Hg, Mo, Zn, Cu, Tl) CO_2 diffuser chimney samples; (f) tephra in marine sediment

cores; and (g) the physical and technical properties of the sediments from expedition 398 of the International Ocean Discovery Program (IODP) [31].

For this study, we used high-resolution 2 m multibeam bathymetry data in our dataset derived from the multibeam bathymetric surveys carried out by the R/V AEGAEO of the Hellenic Centre for Marine Research (HCMR), using a SEABEAM 2120 swath system during three cruises carried out in 2001 and 2006. Our dataset also includes bathymetric data collected in 2015 using the R/V Marcus Langseth's Simrad Kongsberg EM122 12 kHz multibeam echo sounder [32]. During the Oceanographic Cruise POS-510, the AUV Abyss, equipped with a RESON Seabat 7125 multibeam echosounder, acoustic data were collected from inside the Kolumbo volcano and along the flanks. The optical data integrated into our dataset for Kolumbo were collected from the cruise of E/V Nautilus in August 2010 by using ROVs Hercules and Argus. To understand the morphology and construct the lithological map of Kolumbo crater, high-resolution 2 m bathymetry data [33] were combined along with the ROV optical data collected from the cruises of E/V Nautilus in 2010 and 2011. The datasets were combined and analysed by using ArcGIS Pro software to identify the morphology of Kolumbo's crater walls and floor.

2.1. Seafloor Analysis

Semi-automated geomorphological mapping (hereafter stated as SaGM) is a valuable tool for understanding landscape dynamics and landform evolution. It combines automated techniques with expert knowledge to produce detailed and accurate geomorphological maps and allows researchers to perform rapid and efficient identification and classification of landforms and terrain features [34].

SaGM in deep-sea environments has become essential to understanding submarine geomorphological features and processes. It combines advanced remote sensing technologies and machine learning algorithms to efficiently map the seafloor's geomorphology. Several studies have demonstrated the effectiveness of SaGM in deep-sea settings. For example, Harris et al. [35] used multibeam bathymetry data and image analysis to map and classify submarine landforms, revealing the complexity of geomorphological features of underwater environments, and Mayer et al. [36] employed AUV data and automated algorithms to characterise seafloor morphology and identify submarine geological structures. The efficiency of SaGM techniques makes them suitable for surveys of marine environments, contributing to our understanding of submarine geomorphology and geological processes [37]. Moreover, they can improve mapping consistency and reduce manual labour by automating repetitive tasks such as the detection of geomorphological features and classification. However, human expertise remains essential for data interpretation, validation, and improvement [37]. Integrating expert knowledge with automated methods ensures the accuracy and reliability of mapping results, ultimately advancing our knowledge of deep-sea landscapes and their evolution dynamics.

In this study, we employed SaGM to utilise our extensive database and conduct a sea-floor analysis of Kolumbo's crater (Figure 4). High-resolution bathymetry data were inserted into the ArcGIS software and the Digital Elevation Model (DEM) was produced, which served as our basemap. Spatial analysis tools were implemented to generate slope and curvature layers that were overlapped for a more detailed depiction of the seafloor relief. The curvature technique's objective was to highlight areas of rapid change in slope by calculating the associated second derivatives for the terrain model, and then to use the grayscale curvature layer to highlight hill-shaded maps [38]. This technique can be effective when local geological variations in slope are important and in situ observations are sparse. Slope was then classified into five classes to understand terrain stability and potential hazards:

1. 0°–1°: flat to gentle slopes, characterised by terrain with minimal elevation changes, where there may be instability [39];
2. 1°–5°: gentle slopes;
3. 5°–15°: moderately steep slopes that can affect stability;

4. 15°–30°: steep slopes that are more prone to erosion and landslides, especially in areas with loose or unconsolidated materials;
5. >30°: very steep slopes that are highly susceptible to instability and failure.

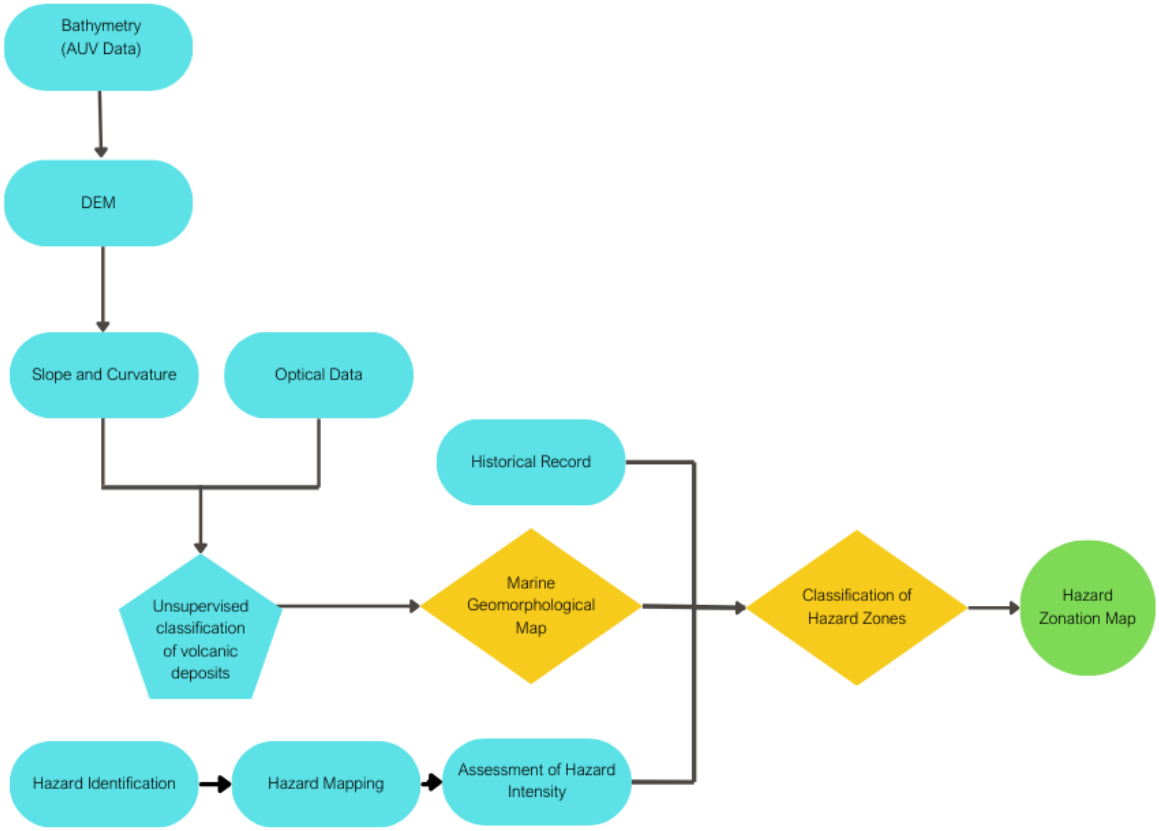

Figure 4. Flowchart showing the applied methodology.

The slope classification was then verified and enriched by optical data from oceanographic expeditions NA007 and NA011 (including ROV videos, photographs) to identify geomorphological characteristics, verify lithological units, and estimate slope stability along Kolumbo's flanks. The historical record was also considered to map the inundation area of Santorini Island during the 1650 CE eruption.

2.2. Hazard Zonation

Volcanic hazard zonation methodologies involve systematic approaches to assess and categorise areas according to the level of risk posed by various types of volcanic hazards. For the hazard zonation near Kolumbo, we based our analysis on data availability and the historical record (Figure 4).

The first step in the volcanic hazard zonation procedure involves identifying potential volcanic hazards associated with the volcanic activity. These hazards may include lava flows, pyroclastic flows, ashfall, lahars, volcanic gases, and volcanic tsunamis [40]. Once hazards are identified, hazard maps are created to delineate areas susceptible to each hazard. These maps are based on geological, historical, and remote sensing data, as well as numerical modelling and expert judgment [40].

In the case of Kolumbo, we identified (i) toxic gases, (ii) ashfall, (iii) pyroclastic flows, and (iv) tsunami generation as the most likely volcanic hazard types. Considering Kolumbo's eruptive history, it is plausible to suggest that a possible eruptive scenario would be a repetition of the 1650 CE eruption. For this study, we consider a 1650 CE-like scenario as the most possible case of eruption since this is the only eruption of Kolumbo that has been documented and studied so far. Kolumbo's eruptive history prior to 1650 CE

is still being investigated. Current conditions suggest that Kolumbo is more active than previously thought. Chrapkiewicz et al. [41] detected a body of mobile magma that has been growing at an average rate of 4 × 106 m^3 per year since the last eruption in 1650 CE. This rate is large enough to counteract the effect of cooling and crystallization; therefore, the seamount poses a serious threat.

In this study, hazard zones were drawn based on historical data of the 1650 CE eruption, the morphology, and the structure of the Kolumbo volcano, derived from multidisciplinary data from oceanographic expeditions and morphological analysis. These hazard zones resulted from a different approach according to which the historical record and qualitative imagery and video data were combined with quantitative high-resolution bathymetry data to generate a slope analysis and an underwater lithological map that helped us characterise areas showing instability. Following the seafloor analysis, the historical data provided us a depiction of the past eruption's effects on Santorini (inundation, toxic gases, ashfall, pyroclastic flows, casualties) and enabled us to define potentially affected zones in the event of a future eruption similar to that of 1650 CE. Hazard intensity was evaluated based on the zones' proximity to the volcano, the hazards that affect them, and the risk to human life [42], and the zones were then classified according to the level of risk they pose. These zones included exclusion, high-risk, and moderate-risk zones. Each zone is associated with proposed mitigation measures and land-use regulations [43].

3. Results

3.1. Seafloor Analysis

The Kolumbo crater is characterised by medium slopes on its western flank, but it is dominated by steep slopes on its N, E, and SE flanks, according to the slope map generated by the DEM (Figure 5a,b). These areas can be considered unstable, and we believe that they pose a significant threat that could trigger a slope failure.

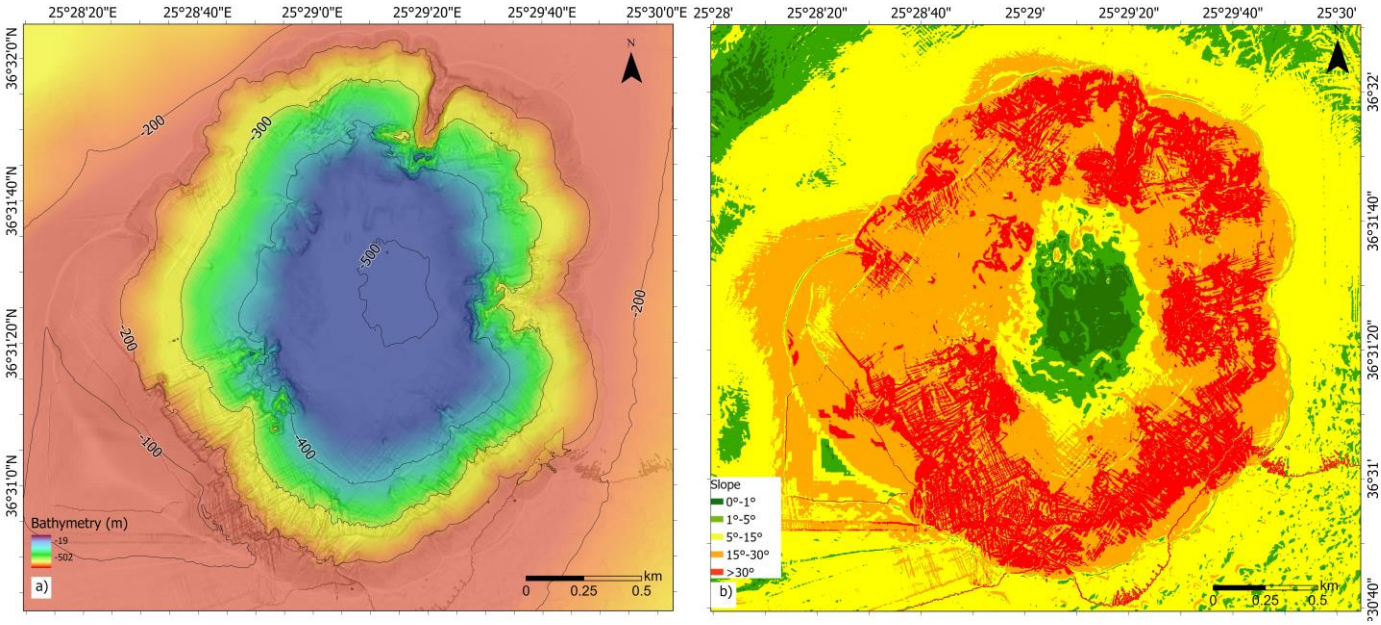

Figure 5. (**a**) Bathymetry map of the study area. (**b**) Slope map of Kolumbo's crater.

The crater exhibits predominant features of highly vesicular pumice and lava deposits along its walls (Figure 6), originating from the 1650 CE eruption [44]. The largest areas of lava flows are located on the northeast and southwest flanks of the crater. The rough terrain observed at the NE area of the crater floor indicates the presence of Kolumbo's active hydrothermal vent field, which was also visible in the ROV video and imagery data. Steeper slopes are evident on the northern, eastern, and southeastern walls, making these

areas susceptible to landslides induced by tectonic activity [45], also visible on the slope map (Figure 5b).

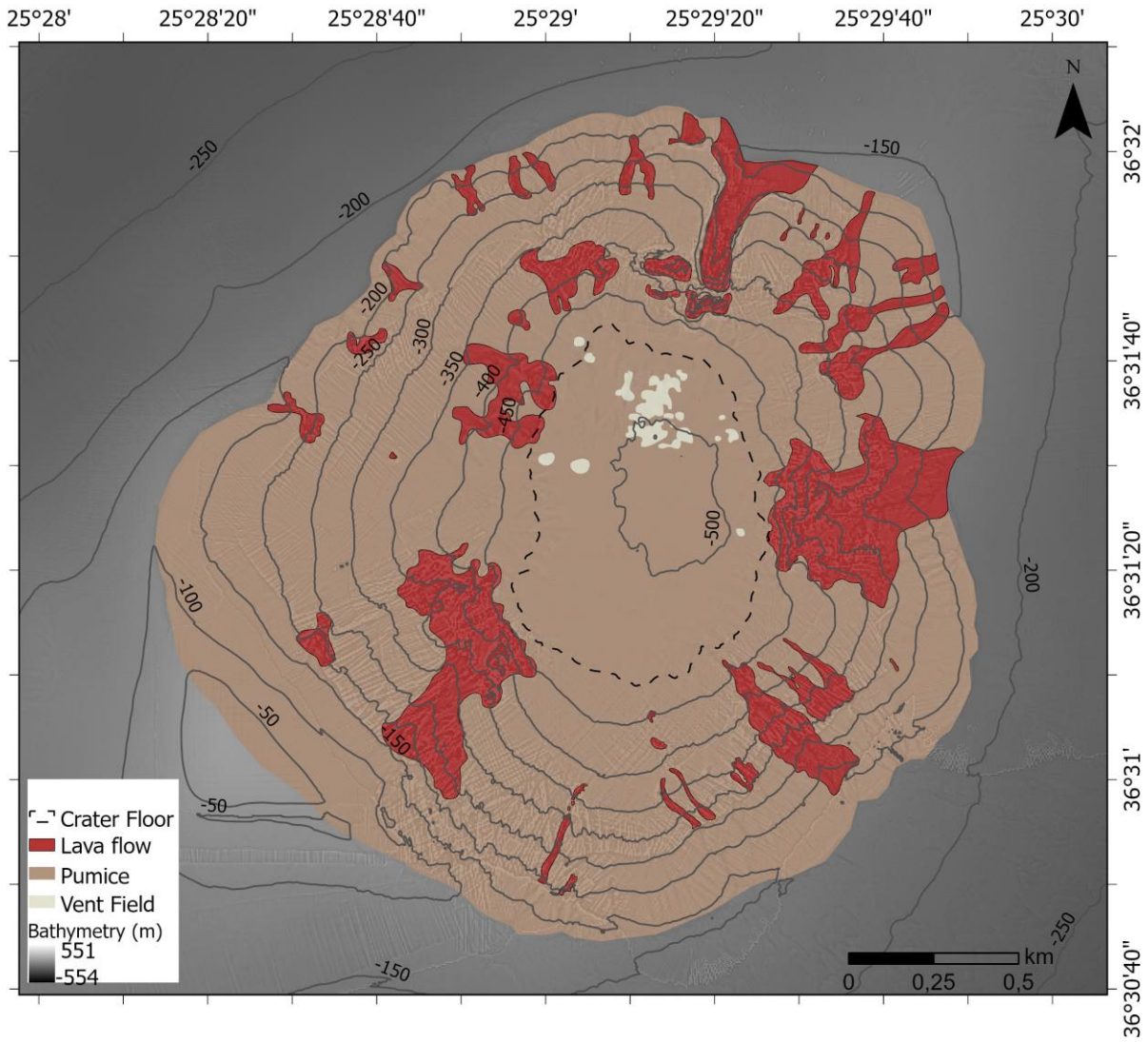

Figure 6. Underwater lithological map of Kolumbo crater. Brown areas are pumice deposits, while lava deposits are shown in red [45] and hydrothermal vents are shown in white.

The detailed analysis of Kolumbo crater's seafloor topography underscores the critical need for a comprehensive geological map. By analysing the morphology, potential hazards within the crater are discerned. The varying degrees of steep slopes, as shown in the slope map (Figure 5b), highlight areas of instability, particularly on the northern, eastern, and southeastern flanks of the crater. These regions, prone to landslides induced by volcanic or tectonic activity, pose significant risks and must be further assessed in terms of landslide susceptibility. Therefore, the lithological map serves as a vital tool for assessing hazards and understanding the geological processes shaping Kolumbo crater's landscape.

3.2. Hazard Zonation

The consequences of the 1650 CE eruption and ensuing tsunami significantly impacted the east coast of Santorini, particularly affecting the towns of Monolithos, Perissa, and Kamari (Figure 7). Historical records document flooding covering up to 2 km^2 of land on the island's eastern coast that resulted in structural damage and erosion of infrastructure [12]. The tsunami model by Karstens et al. [13] was used to identify the areas in danger of

inundation, which were further complemented by the historical observations, and thus the inundation area was drawn (Figure 7).

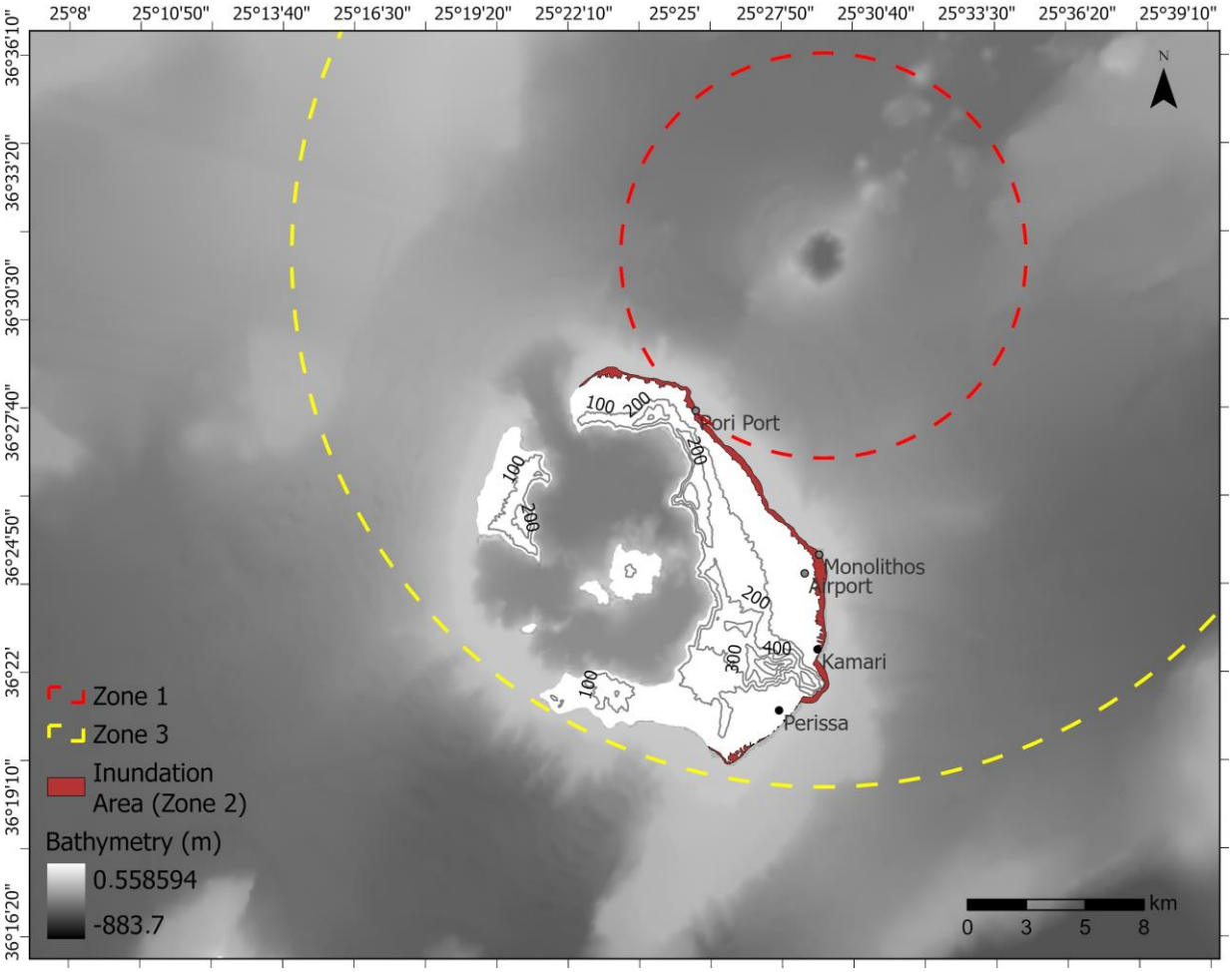

Figure 7. Hazard zonation map showcasing the three preliminary hazard zones in Santorini. The red dashed circle indicates Zone 1 (up to 7 km off Kolumbo), the dark red area is Zone 2 (8 km off Kolumbo's crater) and shows the estimated inundation area based on the simulations of Karstens et al. [13], and the yellow dashed circle is Zone 3 (22 km off Kolumbo). The towns and ports located on the eastern coast were the most affected by the 1650 CE tsunami, according to historical accounts.

Considering the historical record, potential hazards of a Kolumbo eruption include toxic gases, ashfall, pyroclastic flows, and tsunami generation. Given Kolumbo's eruptive history that is known so far and geomorphological characteristics, a plausible scenario is the repetition of the events from the 1650 CE eruption. Such events would likely span a significant amount of time, considering that tectonic activity began approximately a year prior to the eruption and the actual volcanic eruption lasted almost four months (September 1650 to December 1650), with discernible signs of underwater volcanic activity likely preceded by frequent earthquakes followed by discoloured sea surfaces [44]. The recent tsunami simulation model [13] suggests that a tsunami akin to that of 1650 CE could reach the coast of Santorini. Considering the recurrence of events akin to the 1650 CE eruption as a plausible scenario, the following hazard zones can be drawn.

Three hazard zones should be drawn, depending on the degree of the dangers that the above hazards pose to life and their area of impact (Figure 7).

- Zone 1 (up to 7 km off Kolumbo's crater), exclusion zone: This zone includes the offshore area around Kolumbo and reaches up to Santorini's coastline. The zone was drawn based on its nearness to the crater and on the historical accounts of casualties

offshore due to asphyxiation. In this zone, access must be strictly prohibited due to the danger of asphyxiation caused by toxic gas emissions, and the proximity to Kolumbo's crater poses an imminent threat due to pyroclastic flows, ashfall, and potential tsunami generation.

- Zone 2, inundation area (8 km off Kolumbo's crater) high-risk zone: In this zone, which encompasses the coast of Santorini, ashfall and tsunami generation pose significant threats to life. The zone was drawn based on the historical record and the tsunami model by Karstens et al. [13]. It is important to note that the model is based on numerical simulations and was not optimised for inundation; therefore, the acreage of the land is estimated and open to debate. The area should be evacuated to prevent a repetition of the 1650 casualties both inland and offshore, as it contains the most heavily impacted areas of Pori port, Kamari, Monolithos, and Perissa, where water reached up to 2 km^2 inland. Additionally, this zone is extremely close to the only airport on the island, and its location could be compromised due to this proximity in a future eruption, creating problems with transport and isolating the island.
- Zone 3 (22 km off Kolumbo), moderate-risk zone: In this zone, the area is less likely to be affected by a tsunami; however, toxic gas emissions and ashfall still pose a significant hazard that can cause severe health issues as well as destruction of cultivated land and property. According to Fouqué [12], in 1650 CE, the toxic gas emissions reached the shores of Turkey. Considering that the prevailing wind conditions in Santorini indicates that the prevailing wind directions at Thira are the north and northwest (Figure S1) [46], the zone was drawn to include the whole island since, in the case of an eruption scenario similar to the 1650 CE eruption, the winds would carry the toxic gas and ashfall across the island. The use of protective masks, eye protection goggles, and burn-resistant clothes would be necessary to avoid health-associated risks.

3.3. Proposed Measures

Measures prior to the eruption (pre-eruptive phase). Indicators such as seismic activity, enhanced hydrothermal activity, and water discoloration would be expected to last for several days in the vicinity of Kolumbo. During this phase, the Civil Protection Agency should prepare to inform the public of the volcanic activity and possibly begin evacuation of the sick or elderly population since they could possibly not be able escape quickly or autonomously. Access to the vicinity of the volcano must be limited. Scientists should aid the government agency and help with early assessments of hazards and action plans. Continuous seismic activity could cause problems to infrastructure, communications, and the area's road network. This should be taken into consideration, and authorities should implement the relevant protocol for dealing with risks of seismic activity. The areas that are most likely to be affected are located on the east coast of Santorini, and their vulnerability should be assessed thoroughly to consider what should be done in the next phase.

Measures during the eruption (eruptive phase). Following the pre-eruptive events, we can expect dense ash clouds and unpleasant odours arriving inland due to gas emissions [44] while minor earthquakes continue. Seismic activity inside or near the crater could induce landslides on the inner walls due to the steep slopes observed in the crater. Landslides could cause water displacement and thus generate a tsunami. At this phase, access to the offshore area should be prohibited and tide gauges should be put in place to monitor the area for possible tsunami generation. A tsunami watch would be issued if a tsunami may later impact the watch area. The watch may be upgraded to a warning or advisory or cancelled based on updated information. Emergency management officials and the public should be informed and prepared to act with partial or complete evacuation of the eastern coastal area of Santorini and its ports, from the small fishing port of Pori up to the town of Perissa (Figure 7), and initiate the plan for disaster prevention. The hazards of ash fallout and toxic gas emissions should also be considered based on the problems that they cause transportation, where air transportation could be limited or cancelled due to the location of Santorini's only airport in Monolithos; problems with sea transport due to the

ongoing eruption; health implications that derive from the eruption, such as short-term respiratory health issues, including the exacerbation of existing asthma and bronchitis, as well as symptoms such as coughing, breathlessness, chest tightness, and wheezing [47]; and the repercussions on the environment, which could include water contamination, loss of cultivated land, and air pollution. Protective masks and gear should be distributed to avoid asphyxiation and burns. Pyroclastic flows could also cause telecommunication issues due to the destruction of underwater cables, much like the destruction of a vast network of seafloor telecommunication cables by volcanic debris from the Hunga eruption in 2022 that travelled under the sea more than 100 km [8]. The above should be considered by the relevant authorities to plan for alternative uses of transport, the establishment of mobile healthcare facilities, and alternative modes of communication.

4. Discussion

Managing the risks associated with volcanic activity is a complex and interdisciplinary endeavour that requires scientific expertise, risk assessment methodologies, community preparedness, and emergency response planning. Recent studies indicate that the Kolumbo volcano poses a significant threat to the northern and eastern coasts of Santorini, with a potential eruption carrying devastating consequences for the island's population, infrastructure, and environment. Despite the recognised hazard posed by Kolumbo, it has not been adequately addressed in any emergency response or risk mitigation strategies.

Research involving submarine environments faces numerous challenges, primarily due to the inherent difficulty of working in these remote and inaccessible areas. One significant limitation stems from the non-linear nature of optical data, which complicates analysis and interpretation. Additionally, the submarine environment is characterised by dynamic and variable conditions that further complicate data collection and analysis. These challenges necessitated careful consideration and validation of assumptions, as well as the integration of multiple data sources (historical observations, optical data (ROV videos and photos), AUV data) into our methodology to ensure reliable results.

The examination of Kolumbo crater's seafloor topography emphasises the necessity of a comprehensive geological map. Through morphology analysis and a semi-automated approach, significant features and potential hazards were identified—notably, steep slopes on the crater's northern, eastern, and southeastern flanks. These areas require further assessment for landslide susceptibility. The lithological map serves as a crucial tool for visualising the seafloor terrain, assessing hazards, and comprehending the geological processes shaping Kolumbo crater's landscape.

Additionally, the occurrence of volcanic hazards often leads to a complex interplay of cascading risks, where one hazard triggers or exacerbates others, creating a multidimensional crisis scenario. Multi-cascading risks underscore the need for comprehensive risk assessment and management strategies in populated volcanic regions. Volcanic eruptions can unleash a variety of hazards, each with its own destructive potential, but individually they can also act as catalysts to a destructive chain reaction when combined. For instance, the eruption of Mount Pinatubo in 1991 triggered lahars due to heavy rainfall interacting with volcanic debris, which then led to secondary hazards, including river flooding and infrastructure damage [48]. The interconnected nature of volcanic hazards highlights the importance of integrated risk management approaches that account for their cumulative impacts and the potential for cascading effects across various sectors that exacerbate the overall risk [49].

The eruption of Eyjafjallajökull in 2010 demonstrated multi-cascading volcanic hazards on a regional scale. Eyjafjallajökull had been dormant for nearly 200 years when, following about a year of seismic activity, an eruption began on the evening of 20 March 2010 [4]. The eruption fissure was initially about 0.5 km long, located on the northern side of Fimmvörðuháls, east of the Eyjafjallajökull ice cap, and was considered small-scale, with eruptive fissures emitting lava as flows and spatters, as well as growing up ramparts. The eruption ceased on 12 April, but only two days later, on 14 April, an explosive subglacial

eruption started in the caldera beneath the Eyjafjallajökull ice cap. During the next few days, the eruption produced large quantities of fine-grained silicic ash, and the strong northwest winds over Iceland during this event carried it southeast into the airspace of the UK and continental Europe and the North Atlantic area [6]. This caused major disruption to air traffic in northern Europe during the first week of the eruption. Furthermore, airports located as far south as Spain and Morocco had some short closures due to ash also being present in their air spaces. This was the biggest aerial shutdown in Europe since World War II and affected at least ten million passengers worldwide [50] and caused economic losses. Fine volcanic ash particles also posed health risks to humans and animals, leading to respiratory issues and damage to agricultural crops. A recent study of the long-term health effects of the Eyjafjallajökull volcanic eruption indicates that people exposed to a volcanic eruption, especially those most exposed, exhibit increased risk of certain symptoms even 3–4 years after the eruption [5]. Additionally, the melting of glacial ice by the eruption produced lahars that threatened downstream communities and infrastructure, highlighting the interconnected nature of volcanic hazards [51]. The resulting unprecedented disruption to air traffic and the implications for the vulnerability of modern society to even relatively modest eruptions have made Eyjafjallajökull 2010 a landmark event [52]. When Mount Ontake erupted in 2014, the result was a multi-cascading hazard scenario that involved pyroclastic flows, ashfall, and secondary volcanic gas emissions. The sudden release of volcanic gases, including sulphur dioxide and carbon dioxide, posed health risks to nearby populations, leading to respiratory problems and evacuation orders. The volcanic gases also contributed to acid rain, which damaged vegetation and water sources in the surrounding area, exacerbating the environmental impact of the eruption [7].

Kolumbo, like numerous other submarine volcanoes, is often underestimated in terms of its potential threat despite its activity. The consequences of such negligence have been starkly demonstrated, as seen in the events following the 2018 collapse of Anak Krakatau and the subsequent tsunami that claimed over 400 lives [53]. Similarly, the recent eruption of the Hunga Tonga–Hunga Ha'apai submarine volcano in 2022 resulted in at least six fatalities, numerous individuals reported missing, and approximately USD 90.4 million in damages on Tonga island [54]. While research and monitoring of shallow submarine arc volcanoes in the Mediterranean Sea are still in their infancy, efforts have been made to establish in deep-seafloor observatories to monitor submarine volcanoes over extended periods. Notable examples include the Azores node of the European Multidisciplinary Seafloor and Water Column Observatory [55], the Axial Seamount in the NE Pacific as part of the U.S. National Science Foundation (NSF)-funded Ocean Observatories Initiative (OOI) Cabled Array, Ocean Networks Canada's cabled observatory at Endeavour Ridge [56], and the Mayotte deep-sea eruption observatory in the North Mozambique Channel, established by France [57]. These observatories have proven effective in tracking changes in submarine volcanic dynamics. For example, the 2015 eruption at Axial Seamount was accurately forecasted within a one-year window based on volcanic deformation and was monitored in real time by the OOI Cabled Array [58]. Presently, deformation and seismic monitoring techniques are being employed to predict future eruptions, with forecasts extending over the next 4 to 9 years [59].

We believe it is imperative to develop a comprehensive strategy that includes hazard and risk assessments, as well as mitigation measures, to effectively manage the risks associated with Kolumbo. Active monitoring of the volcano is crucial for gathering essential information about its evolution, mechanisms, and early signs of potential eruptions to inform the public promptly. However, monitoring submarine volcanoes presents unique challenges, including the difficulty of implementing and maintaining underwater monitoring systems over extended periods and developing suitable instruments for this purpose, although notable efforts have been made globally in recent years.

Currently, Kolumbo is being monitored using an underwater observatory called SANTORY (SANTORini's seafloor volcanic observatorY), a collaborative research project involving international institutions and universities funded by the Hellenic Foundation for

Research and Innovation. The project aims to understand the connections between deep-seated geological processes, associated risks, and hydrothermal activity. Our international research team employs state-of-the-art technology for in situ monitoring, combined with discrete sampling and measurements. Thus far, we have conducted three oceanographic expeditions funded by the municipality of Thera–Santorini, during which we deployed and maintained the seafloor observatory, conducted various measurements within Kolumbo's crater using innovative sensors, continuously monitored the active hydrothermal vent field with optical cameras, and conducted real-time measurements of radioactivity using advanced instruments.

5. Conclusions

Managing the risks associated with volcanic activity requires a multidisciplinary approach encompassing scientific expertise, risk assessment methodologies, community preparedness, and emergency response planning. The recent events of volcanic eruptions both to terrestrial and submarine volcanoes highlight the need for the development of risk mitigation strategies and continuous monitoring to detect early signs of volcanic activity. Recent studies highlight the significant threat posed by the Kolumbo volcano, yet this remains inadequately addressed. This study presents preliminary hazard zonation results for Santorini Island, utilising semi-automated techniques and optical data to characterise Kolumbo's crater structure and risks. Steep slopes in the crater raise concerns for flank collapse and potential tsunami generation, requiring further research on landslide susceptibility.

The ongoing observation of Kolumbo's activity yields invaluable data that can assist government agencies and local communities in formulating strategies and preparing for potential crises. The unique time-series data collected by SANTORY's instruments complements existing databases compiled during numerous oceanographic expeditions and provides essential insights into Kolumbo's activity and dynamics. This knowledge is crucial for conducting hazard assessments, evaluating volcanic risks, and safeguarding vulnerable communities near Kolumbo. By studying volcanic systems over extended periods, we enhance our ability to identify recurring patterns and unusual occurrences, ultimately improving our capacity to forecast eruptions and mitigate their impact.

Supplementary Materials: The following supporting information can be downloaded at: https://www.mdpi.com/article/10.3390/geohazards5030041/s1, Figure S1: Rose diagram showing the prevailing wind conditions in Santorini based on observations from 1 January 2000 to 24 July 2024 [47,60,61].

Author Contributions: Conceptualization, A.K. and P.N.; methodology, A.K.; software, A.K.; validation, A.K., P.N. and K.P.; formal analysis, A.K.; investigation, A.K.; resources, A.K. and P.N.; data curation, A.K.; writing—original draft preparation, A.K.; writing—review and editing, A.K., P.N. and K.P.; visualization, A.K.; supervision, P.N. and K.P.; project administration, P.N.; funding acquisition, P.N. All authors have read and agreed to the published version of the manuscript.

Funding: This research was funded by the SANTORY program, funded by the Hellenic Foundation for Research and Innovation (HFRI) (grant number 1850) in the framework of the "1st Announcement of Research Projects HFRI for Faculty Members and researchers and the supply of high-value research equipment", with a duration of three years. Fieldwork activities were funded by Sorbonne University Abu Dhabi research program 3389.

Data Availability Statement: This research used data collected by E/V Nautilus expeditions NA007, NA011, and NA014, which were supported by NOAA Ocean Exploration. The data used are publicly available upon request. Data can be requested at https://nautiluslive.org/science/data-management, accessed on 16 June 2023.

Acknowledgments: Special thanks to the captain and crew of E/V Nautilus, the Nautilus Corps of Exploration, the Ocean Exploration Trust, and all who supported the expedition from the shore, as well as all IODP scientists from Expedition 398. We would like to extend our sincere gratitude to the anonymous reviewers for their constructive feedback and insightful comments, which greatly

contributed to the improvement of this manuscript. We also wish to thank Jens Karstens for his invaluable help and for providing the tsunami simulation data. Additionally, we are deeply grateful to the chief scientists of IODP Expedition 398, Tim Druitt and Steffen Kutterolf, for their support and contributions to this research.

Conflicts of Interest: The authors declare no conflicts of interest. The funders had no role in the design of the study; in the collection, analyses, or interpretation of data; in the writing of the manuscript; or in the decision to publish the results.

References

1. Fontaine, F.R.; Roult, G.; Michon, L.; Barruol, G.; Muro, A.D. The 2007 Eruptions and Caldera Collapse of the Piton de La Fournaise Volcano (La Réunion Island) from Tilt Analysis at a Single Very Broadband Seismic Station. *Geophys. Res. Lett.* **2014**, *41*, 2803–2811. [CrossRef]
2. UNISDR (United Nations International Strategy for Disaster Reduction). *Sendai Framework for Disaster Risk Reduction 2015–2030*; UNISDR: Geneva, Switzerland, 2015.
3. Lavigne, F.; De Coster, B.; Juvin, N.; Flohic, F.; Gaillard, J.-C.; Texier, P.; Morin, J.; Sartohadi, J. People's Behaviour in the Face of Volcanic Hazards: Perspectives from Javanese Communities, Indonesia. *J. Volcanol. Geotherm. Res.* **2008**, *172*, 273–287. [CrossRef]
4. Sigmundsson, F.; Hreinsdóttir, S.; Hooper, A.; Árnadóttir, T.; Pedersen, R.; Roberts, M.J.; Óskarsson, N.; Auriac, A.; Decriem, J.; Einarsson, P.; et al. Intrusion Triggering of the 2010 Eyjafjallajökull Explosive Eruption. *Nature* **2010**, *468*, 426–430. [CrossRef] [PubMed]
5. Hlodversdottir, H.; Petursdottir, G.; Carlsen, H.K.; Gislason, T.; Hauksdottir, A. Long-Term Health Effects of the Eyjafjallajökull Volcanic Eruption: A Prospective Cohort Study in 2010 and 2013. *BMJ Open* **2016**, *6*, e011444. [CrossRef] [PubMed]
6. Laeger, K.; Petrelli, M.; Andronico, D.; Misiti, V.; Scarlato, P.; Cimarelli, C.; Taddeucci, J.; Del Bello, E.; Perugini, D. High-Resolution Geochemistry of Volcanic Ash Highlights Complex Magma Dynamics during the Eyjafjallajökull 2010 Eruption. *Am. Mineral.* **2017**, *102*, 1173–1186. [CrossRef]
7. Yamaoka, K.; Geshi, N.; Hashimoto, T.; Ingebritsen, S.E.; Oikawa, T. Special Issue "The Phreatic Eruption of Mt. Ontake Volcano in 2014". *Earth Planets Space* **2016**, *68*, 175. [CrossRef]
8. Clare, M.A.; Yeo, I.A.; Watson, S.; Wysoczanski, R.; Seabrook, S.; Mackay, K.; Hunt, J.E.; Lane, E.; Talling, P.J.; Pope, E.; et al. Fast and Destructive Density Currents Created by Ocean-Entering Volcanic Eruptions. *Science* **2023**, *381*, 1085–1092. [CrossRef]
9. Hellenic Statistical Authority. Government of Greece 2021. Available online: www.statistics.gr (accessed on 7 September 2023).
10. Dominey-Howes, D.; Minos-Minopoulos, D. Perceptions of Hazard and Risk on Santorini. *J. Volcanol. Geotherm. Res.* **2004**, *137*, 285–310. [CrossRef]
11. Rizzo, A.L.; Caracausi, A.; Chavagnac, V.; Nomikou, P.; Polymenakou, P.N.; Mandalakis, M.; Kotoulas, G.; Magoulas, A.; Castillo, A.; Lampridou, D. Kolumbo Submarine Volcano (Greece): An Active Window into the Aegean Subduction System. *Sci. Rep.* **2016**, *6*, 28013. [CrossRef]
12. Fouqué, F. *Santorin et ses Éruptions*; Masson & Cie: Paris, France, 1879.
13. Karstens, J.; Crutchley, G.J.; Hansteen, T.H.; Preine, J.; Carey, S.; Elger, J.; Kühn, M.; Nomikou, P.; Schmid, F.; Dalla Valle, G.; et al. Cascading Events during the 1650 Tsunamigenic Eruption of Kolumbo Volcano. *Nat. Commun.* **2023**, *14*, 6606. [CrossRef]
14. McKenzie, D. Active Tectonics of the Mediterranean Region. *Geophys. J. Int.* **1972**, *30*, 109–185. [CrossRef]
15. Pichon, X.L.; Angelier, J. The Hellenic Arc and Trench System: A Key to the Neotectonic Evolution of the Eastern Mediterranean Area. *Tectonophysics* **1979**, *60*, 1–42. [CrossRef]
16. Druitt, T.H.; Edwards, L.; Mellors, R.M.; Pyle, D.M.; Sparks, R.S.J.; Lanphere, M.; Davies, M.; Barreirio, B. *Santorini Volcano: Geological Society [London] Memoir*; The Geological Society: London, UK, 1999; Volume 19, 165p.
17. Nomikou, P.; Hübscher, C.; Carey, S. The Christiana–Santorini–Kolumbo Volcanic Field. *Elements* **2019**, *15*, 171–176. [CrossRef]
18. Preine, J.; Karstens, J.; Hübscher, C.; Nomikou, P.; Schmid, F.; Crutchley, G.J.; Druitt, T.H.; Papanikolaou, D. Spatio-Temporal Evolution of the Christiana-Santorini-Kolumbo Volcanic Field, Aegean Sea. *Geology* **2022**, *50*, 96–100. [CrossRef]
19. Nomikou, P.; Hübscher, C.; Ruhnau, M.; Bejelou, K. Tectono-Stratigraphic Evolution through Successive Extensional Events of the Anydros Basin, Hosting Kolumbo Volcanic Field at the Aegean Sea, Greece. *Tectonophysics* **2016**, *671*, 202–217. [CrossRef]
20. Bruins, H.J.; MacGillivray, J.A.; Synolakis, C.E.; Benjamini, C.; Keller, J.; Kisch, H.J.; Klügel, A.; Van Der Plicht, J. Geoarchaeological Tsunami Deposits at Palaikastro (Crete) and the Late Minoan IA Eruption of Santorini. *J. Archaeol. Sci.* **2008**, *35*, 191–212. [CrossRef]
21. Nomikou, P.; Polymenakou, P.N.; Rizzo, A.L.; Petersen, S.; Hannington, M.; Kilias, S.P.; Papanikolaou, D.; Escartin, J.; Karantzalos, K.; Mertzimekis, T.J.; et al. SANTORY: SANTORini's Seafloor Volcanic ObservatorY. *Front. Mar. Sci.* **2022**, *9*, 796376. [CrossRef]
22. Piper, D.J.W.; Pe-Piper, G.; Perissoratis, C.; Anastasakis, G. Distribution and Chronology of Submarine Volcanic Rocks around Santorini and Their Relationship to Faulting. *Geol. Soc. Lond. Spéc. Publ.* **2007**, *291*, 99–111. [CrossRef]
23. Hübscher, C.; Ruhnau, M.; Nomikou, P. Volcano-Tectonic Evolution of the Polygenetic Kolumbo Submarine Volcano/Santorini (Aegean Sea). *J. Volcanol. Geotherm. Res.* **2015**, *291*, 101–111. [CrossRef]
24. Nomikou, P.; Carey, S.; Papanikolaou, D.; Croff Bell, K.; Sakellariou, D.; Alexandri, M.; Bejelou, K. Submarine Volcanoes of the Kolumbo Volcanic Zone NE of Santorini Caldera, Greece. *Glob. Planet. Chang.* **2012**, *90–91*, 135–151. [CrossRef]

25. Karstens, J.; Preine, J.; Crutchley, G.J.; Kutterolf, S.; Van Der Bilt, W.G.M.; Hooft, E.E.E.; Druitt, T.H.; Schmid, F.; Cederstrøm, J.M.; Hübscher, C.; et al. Revised Minoan Eruption Volume as Benchmark for Large Volcanic Eruptions. *Nat. Commun.* **2023**, *14*, 2497. [CrossRef] [PubMed]
26. Klaver, M.; Carey, S.; Nomikou, P.; Smet, I.; Godelitsas, A.; Vroon, P. A Distinct Source and Differentiation History for Kolumbo Submarine Volcano, Santorini Volcanic Field, Aegean Arc. *Geochem. Geophys. Geosyst.* **2016**, *17*, 3254–3273. [CrossRef] [PubMed]
27. Kilias, S.P.; Nomikou, P.; Papanikolaou, D.; Polymenakou, P.N.; Godelitsas, A.; Argyraki, A.; Carey, S.; Gamaletsos, P.; Mertzimekis, T.J.; Stathopoulou, E.; et al. New Insights into Hydrothermal Vent Processes in the Unique Shallow-Submarine Arc-Volcano, Kolumbo (Santorini), Greece. *Sci. Rep.* **2013**, *3*, 2421. [CrossRef] [PubMed]
28. Polymenakou, P.N.; Nomikou, P.; Hannington, M.; Petersen, S.; Kilias, S.P.; Anastasiou, T.I.; Papadimitriou, V.; Zaka, E.; Kristoffersen, J.B.; Lampridou, D.; et al. Taxonomic Diversity of Microbial Communities in Sub-Seafloor Hydrothermal Sediments of the Active Santorini-Kolumbo Volcanic Field. *Front. Microbiol.* **2023**, *14*, 1188544. [CrossRef] [PubMed]
29. Carey, S.N.; Bell, K.L.C.; Rosi, M.; Marani, M.; Nomikou, P.; Walker, S.L.; Faure, K.; Kelly, J. Submarine Volcanoes of the Aeolian Arc, Tyrrhenian Sea. In *New Frontiers in Ocean Exploration: The E/V Nautilus and NOAA Ship Okeanos Explorer 2011 Field Season*; Bell, K.L.C., Elliott, K., Martinez, C., Fuller, S.A., Eds.; Oceanography: Rockville, MD, USA, 2012.
30. Siebert, L.; Simkin, T.; Kimberly, P. *Volcanoes of the World*, 3rd ed.; University of California Press: Berkeley, CA, USA, 2010.
31. Druitt, T.H.; Kutterolf, S.; Ronge, T.A.; The Expedition 398 Scientists. *Expedition 398 Preliminary Report: Hellenic Arc Volcanic Field*; International Ocean Discovery Program: College Station, TX, USA, 2024. [CrossRef]
32. Hooft, E.E.E.; Nomikou, P.; Toomey, D.R.; Lampridou, D.; Getz, C.; Christopoulou, M.-E.; O'Hara, D.; Arnoux, G.M.; Bodmer, M.; Gray, M.; et al. Backarc Tectonism, Volcanism, and Mass Wasting Shape Seafloor Morphology in the Santorini-Christiana-Amorgos Region of the Hellenic Volcanic Arc. *Tectonophysics* **2017**, *712–713*, 396–414. [CrossRef]
33. Hannington, M.D. (Ed.) *RV POSEIDON Fahrtbericht/Cruise Report POS510—ANYDROS: Rifting and Hydrothermal Activity in the Cyclades Back-arc Basin, Catania (Italy)—Heraklion (Greece)*; GEOMAR Report, N. Ser. 043; GEOMAR Helmholtz-Zentrum für Ozeanforschung: Kiel, Germany, 2018; 56 + Appendix pp. [CrossRef]
34. Quesada-Román, A.; Peralta-Reyes, M. Geomorphological Mapping Global Trends and Applications. *Geographies* **2023**, *3*, 610–621. [CrossRef]
35. Harris, P.T.; Macmillan-Lawler, M.; Rupp, J.; Baker, E.K. Geomorphology of the Oceans. *Mar. Geol.* **2014**, *352*, 4–24. [CrossRef]
36. Mayer, L.; Jakobsson, M.; Allen, G.; Dorschel, B.; Falconer, R.; Ferrini, V.; Lamarche, G.; Snaith, H.; Weatherall, P. The Nippon Foundation—GEBCO Seabed 2030 Project: The Quest to See the World's Oceans Completely Mapped by 2030. *Geosciences* **2018**, *8*, 63. [CrossRef]
37. Roche, M.; Lamarche, G.; Le Gonidec, Y.; Lucieer, V.; Weber, T.; Heffron, E. Semi-automated benthic habitat mapping using MBES and AUV data: A case study from the Bounty Trough, New Zealand. *Geosciences* **2020**, *10*, 228.
38. Micallef, A.; Krastel, S.; Savini, A. (Eds.) *Submarine Geomorphology*; Springer Geology; Springer International Publishing: Cham, Switzerland, 2018. [CrossRef]
39. Kennelly, P.J. Terrain Maps Displaying Hill-Shading with Curvature. *Geomorphology* **2008**, *102*, 567–577. [CrossRef]
40. Ye, Y.; et al. Submarine Landslides. In *Marine Geo-Hazards in China*; Elsevier: Amsterdam, The Netherlands, 2017; pp. 179–267. [CrossRef]
41. *The Encyclopedia of Volcanoes*; Elsevier: Amsterdam, The Netherlands, 2015. [CrossRef]
42. Chrapkiewicz, K.; Paulatto, M.; Heath, B.A.; Hooft, E.E.E.; Nomikou, P.; Papazachos, C.B.; Schmid, F.; Toomey, D.R.; Warner, M.R.; Morgan, J.V. Magma Chamber Detected Beneath an Arc Volcano With Full-Waveform Inversion of Active-Source Seismic Data. *Geochem. Geophys. Geosyst* **2022**, *23*, e2022GC010475. [CrossRef]
43. Marzocchi, W.; Woo, G. Probabilistic Eruption Forecasting and the Call for an Evacuation. *Geophys. Res. Lett.* **2007**, *34*, 2007GL031922. [CrossRef]
44. Marzocchi, W.; Bebbington, M.S. Probabilistic Eruption Forecasting at Short and Long Time Scales. *Bull. Volcanol.* **2012**, *74*, 1777–1805. [CrossRef]
45. Cantner, K.; Carey, S.; Nomikou, P. Integrated Volcanologic and Petrologic Analysis of the 1650AD Eruption of Kolumbo Submarine Volcano, Greece. *J. Volcanol. Geotherm. Res.* **2014**, *269*, 28–43. [CrossRef]
46. Katsigera, A.; Nomikou, P.; Team, S. Addressing the Hazard Risks of Kolumbo Submarine Volcano (Santorini, Greece). In Proceedings of the International Conference on Humanitarian Krisis Management 2023, International Hellenic University, Thessaloniki, Greece, 14–16 October 2023.
47. Iowa Environmental Mesonet. Iowa State University. 2024. Available online: http://mesonet.agron.iastate.edu/ (accessed on 24 July 2024).
48. Horwell, C.J.; Baxter, P.J. The Respiratory Health Hazards of Volcanic Ash: A Review for Volcanic Risk Mitigation. *Bull. Volcanol.* **2006**, *69*, 1–24. [CrossRef]
49. Scarpa, R. *Monitoring and Mitigation of Volcano Hazards*; Springer: Berlin/Heidelberg, Germany, 1996. [CrossRef]
50. Tilloy, A.; Malamud, B.D.; Winter, H.; Joly-Laugel, A. A Review of Quantification Methodologies for Multi-Hazard Interrelationships. *Earth-Sci. Rev.* **2019**, *196*, 102881. [CrossRef]
51. Gudmundsson, M.T. Hazards from Lahars and Jökulhlaups. In *The Encyclopedia of Volcanoes*; Elsevier: Amsterdam, The Netherlands, 2015; pp. 971–984. [CrossRef]

52. Petersen, G.N. A Short Meteorological Overview of the Eyjafjallajökull Eruption 14 April–23 May 2010. *Weather* **2010**, *65*, 203–207. [CrossRef]
53. BNPB-National Disaster Management Agency, Tsunami Selat Sunda. Available online: https://reliefweb.int/report/indonesia/indonesia-sunda-straights-tsunami-emergency-plan-action-mdrid014 (accessed on 8 March 2019).
54. The World Bank and the Global Facility for Disaster Reduction and Recovery. *The January 15, 2022 Hunga Ton-ga-HungaHa'apai Eruption and Tsunami, Tonga: Global Rapid Post Disaster Damage Estimation (Grade) Report*; International Bank for Reconstruction and Development/TheWorldBank: Washington, DC, USA, 2022; Available online: https://shorturl.at/tBJY3 (accessed on 5 May 2023).
55. Escartin, J.; Barreyre, T.; Cannat, M.; Garcia, R.; Gracias, N.; Deschamps, A.; Salocchi, A.; Sarradin, P.-M.; Ballu, V. Hydrothermal Activity along the Slow-Spreading Lucky Strike Ridge Segment (Mid-Atlantic Ridge): Distribution, Heatflux, and Geological Controls. *Earth Planet. Sci. Lett.* **2015**, *431*, 173–185. [CrossRef]
56. Kelley, D.S.; Delaney, J.R.; Juniper, S.K. Establishing a New Era of Submarine Volcanic Observatories: Cabling Axial Seamount and the Endeavour Segment of the Juan de Fuca Ridge. *Mar. Geol.* **2014**, *352*, 426–450. [CrossRef]
57. Feuillet, N.; Jorry, S.; Crawford, W.C.; Deplus, C.; Thinon, I.; Jacques, E.; Saurel, J.M.; Lemoine, A.; Paquet, F.; Satriano, C.; et al. Birth of a Large Volcanic Edifice Offshore Mayotte via Lithosphere-Scale Dyke Intrusion. *Nat. Geosci.* **2021**, *14*, 787–795. [CrossRef]
58. Nooner, S.L.; Chadwick, W.W. Inflation-Predictable Behavior and Co-Eruption Deformation at Axial Seamount. *Science* **2016**, *354*, 1399–1403. [CrossRef] [PubMed]
59. Chadwick, W.W.; Wilcock, W.S.D.; Nooner, S.L.; Beeson, J.W.; Sawyer, A.M.; Lau, T.-K. Geodetic Monitoring at Axial Seamount Since Its 2015 Eruption Reveals a Waning Magma Supply and Tightly Linked Rates of Deformation and Seismicity. *Geochem. Geophys. Geosyst.* **2022**, *23*, e2021GC010153. [CrossRef]
60. How Slope Works, ArcGIS Pro Documentation. Available online: https://pro.arcgis.com/en/pro-app/latest/tool-reference/3d-analyst/how-slope-works.htm (accessed on 24 July 2024).
61. Slope (Spatial Analyst), ArcGIS Pro Documentation. Available online: https://pro.arcgis.com/en/pro-app/latest/tool-reference/spatial-analyst/slope.htm (accessed on 24 July 2024).

Disclaimer/Publisher's Note: The statements, opinions and data contained in all publications are solely those of the individual author(s) and contributor(s) and not of MDPI and/or the editor(s). MDPI and/or the editor(s) disclaim responsibility for any injury to people or property resulting from any ideas, methods, instructions or products referred to in the content.